Supplementary Materials

For

The Oestrogen Pathway Underlies the Evolution of Exaggerated Male Cranial Shapes in *Anolis* Lizards

Thomas J. Sanger, Susan M. Seav, Masayoshi Tokita, R. Brian Langerhans, Jonathan B. Losos, Arhat Abzhanov

Table of Contents for Supplementary Materials

Supplementary Methods

(a) Species selection and morphological measurements

We compared cranial and post-cranial levels of sexual dimorphism for 30 *Anolis* species using a combination of linear and geometric morphometrics [1]. We obtained all specimens from the Museum of Comparative Zoology at Harvard University. Sexual dimorphism in head shape was calculated following Sanger et al. [2]. Briefly, we placed 24 landmarks across the dorsal surface of dried skulls for males and females of 30 anole species with varying levels of sexual dimorphism using TPSdig2 [3]. All subsequent geometric morphometric analyses were performed in MorphoJ [4]. We calculated the average values of landmark coordinates for each species removing the effects of position, orientation, and scale from the data [1]. Procrustes superimposition accounted for "object symmetry" of the skull by reflecting lateral landmarks across the midline to find an average landmark position [5]. We tested for allometric scaling using a multivariate regression of shape data on centroid size, the preferred measure of size in geometric morphometrics, but allometry was not found to significantly contribute to variation in head shape among this sample (permutation test p-value = 0.078). Principal component analysis was then conducted on shape variables to extract the primary axes of skull shape variation.

We collected postcranial measurements of alcohol-preserved specimens of the same 30 species using 1) a 3D coordinate digitizer (Polhemus Liberty, Colchester, Vermont) to measure five linear measurements (snout to vent length [SVL], hindlimb length, forelimb length, pectoral width, and pelvic width), and 2) a digital scanner to capture images for counting the number of foot and hand lamellae. We log-transformed all variables and calculated size-corrected values for the six focal traits using residuals from linear regression on SVL, the standard measurement of body size in herpetological studies. We then used principal component analysis to extract the primary axes of postcranial shape variation. Following Sanger et al. [2], we calculated sexual dimorphism for both cranial and post-cranial date sets as the Euclidean distance between males and females of each species taking into account all significant PC axes. For both cranial and post-cranial datasets, sample sizes for each sex of each species is given in Table S4.

We compared gene expression levels between males and females of three species, *A. carolinensis*, *A. sagrei*, and *A. cristatellus*. Of the species within the *carolinensis* clade, *A. carolinensis* was chosen because of its growing genomic resources [6]. Gene expression data for *A. carolinensis* was collected in 2010-2011 from both wild-caught (sub-adult and adult, Reserve, LA) and captive-bred (juvenile) individuals. Gene expression for *A. sagrei* and *A. cristatellus* was assessed in 2012 and 2013 using lizards from introduced populations in and around Miami, FL. These species have independently converged on the short-faced morphology [7] and relatively low levels of sexual dimorphism [2]. Juvenile lizards were collected following hatching from eggs incubated at Harvard University. Detailed descriptions of egg incubation and *Anolis* husbandry can be found elsewhere [8].

(b) Proliferation assay, histology, and pulse labeling

To obtain quality sections of the adult anole cranium we decalcified specimens at room temperature for six to ten days in 0.5M EDTA. We then embedded the specimens in OCT and obtained 12μm sagittal sections through cryosectioning. To visualize cellular morphology we stained sections with hematoxylin and eosin. We assessed patterns of chondrocyte proliferation in the adult nasal septum of male *A. carolinensis* using the Click-it EdU Alexa Fluo 488 Imaging Kit following manufacturer's protocols (0.2ml IP injection, 20mg/ml EDU, six hour pulse, Life Technologies Inc.).

To assess ossification patterns associated within the elongating anole face we administered calcein (green fluorescence) 30 days prior to sacrifice followed by alizarin red complexone (red fluorescence) 24 hours prior to sacrifice. The distance between green and red labels, therefore, represents the amount of growth that occurred for each skeletal element between pulses. We compared facial elongation rates between adult male and adult female green anoles using a two-tailed t-test on growth of the premaxilla.

(c) Cloning and in situ hybridization (ISH)

To prepare riboprobes for ISH we cloned 500-1000 base pair fragments of the hormonal receptors from embryonic *A. carolinensis* cDNA (*ar*: ENSACAG00000009496; *igfr1*: ENSACAG00000008089; *erα*: ENSACAT00000006243; *erβ*: ENSACAG00000015814; *ghr*: ENSACAG00000010633; *pth1r*: ENSACAG00000004743). Species-specific primers targeting these molecules were designed from the green anole genome sequences [6]. Orthology was determined using BLAST analysis. We performed ISH on cryo- sections using dig-labeled riboprobes following Abzhanov 2009 with the exception that NBT/BCIP color development occurred in 10% polyvinyl alcohol to reduce background alkaline-phosphatase activity.

(d) Tissue collection and quantitative real-time PCR (rtPCR)

We compared relative gene expression between the sexes and between stages using rtPCR. To collect RNA from the elongating face we separated the skin from the skeletal tissue anterior to the orbit. The skeletal tissue was then dissected from the remainder of the cranium, preserved in RNAlater (Qiagen), and stored in liquid nitrogen. We extracted facial RNA using a Tissuelyser (Qiagen) and RNeasy minikit (Qiagen) and prepared cDNA using the treated with Turbo-DNase (Applied Biosystems) and generated cDNA using M-MuLV reverse transcriptase with poly-A primers (New England Biolabs). Gene expression analysis for *A. sagrei* and *A. cristatellus* were performed as described above except that we generated cDNA using the qScript cDNA Synthesis Kit (Quanta Biosciences). All primers were designed to genomic sequences from *A. carolinensis* [*6*] unless otherwise noted (Table S8). In addition to hormonal receptor primers were designed to nine signaling, patterning, and skeletogenic molecules: *bmp4*: ENSACAG00000017900; *bmp2*: ENSACAG00000003113; *msx2*: ENSACAG00000015018; *ihh*: ENSACAG00000005172; *tgfβr2*: ENSACAG00000014301; *dkk3*: ENSACAG00000004940; *spp1*: ENSACAG00000012670; *col I*:

ENSACAG00000005084; *col II*: ENSACAG00000016827. All genes used in comparative analyses were cloned from post-embryonic facial cDNA to verify their sequence similarity. All primers flank an exon boundary to control for genomic DNA contamination. Primer sequences for *src* and *cbp1* were donated by the Wade Lab (Michigan State University). Gene expression levels were assayed using an Eppendorf Mastercycler using SYBR green (Kapa Bio-systems) with 40 cycles of amplification. Gene expression was assayed in triplicate for each sample and normalized for *gapdh* and β-actin. Finally, we analyzed the expression data using the comparative CT method [9].

Supplementary Figures

Figure S1: Developmental timing of facial length dimorphism. Most anole species develop dimorphism using a common developmental (allometric) strategy where males (solid line) and females (dashed line) diverge during a discrete period of time early in post-hatching ontogeny. However, the *carolinensis* clade evolved its extreme facial length dimorphism through the evolution of a novel developmental strategy, diverging late in life following sexual maturity. Note that these plots contrast facial length elongation with growth in body size, not absolute measures of growth rate as measured in our analyses presented here. See Sanger et al. [2] for further details of the comparative morphometric analyses.

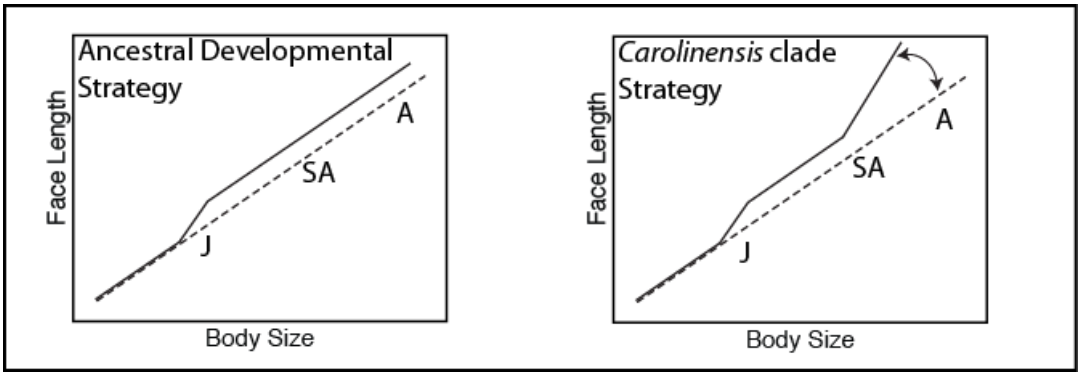

Figure S2: Consistent with previous morphometric analyses [2], the primary axis of cranial diversity among anoles is facial length and, to a lesser extent, skull width. The landmarks used for morphometric analysis are illustrated on a representative skull of *A. porcatus* (A). The primary axis of skull shape variation (PC1, 47.7% of the cranial variation) is summarized by variation in facial length and cranial width (B; grey wire diagram represents shape average skull in our sample, the black wire diagram represents the positive deviation along PC1). (C) Plot of cranial versus post-cranial dimorphism for a sample of 30 *Anolis* species. The relatively low correlation between the two values (R^2 = 0.225, p-value derived from a phylogenetic regression) illustrates that dimorphism in the head and body have evolved somewhat independently. Stars denote species within the *carolinensis* clade, illustrating that their post-cranial dimorphism does not consistently reach extreme levels of dimorphism compared to other anole species despite their extreme cranial dimorphism [2].

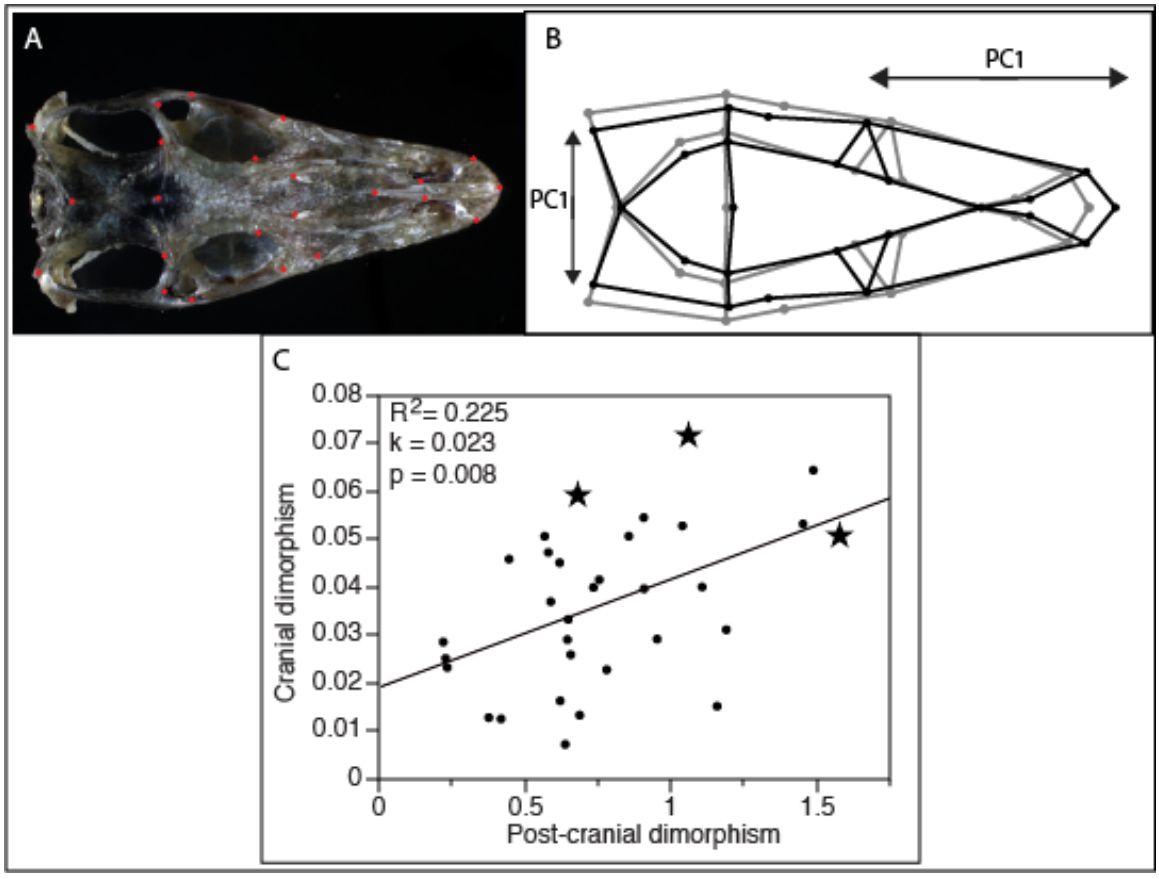

Figure S3: Ossification patterns associated with facial elongation of *A. carolinensis*. In anoles all facial outgrowth occurs anterior to the orbit (OR). In contrast to murine facial elongation, which is localized to the anterior side of the nasal-frontal suture, measureable amounts of facial elongation occur across the anole face (arrows): on the anterior and posterior sides of the frontal (FR)-nasal (NA)-premaxilla (PM) suture, the anterior nasal bone, and at the maxilla-premaxilla suture. But despite this difference among distantly related species, the greatest rates of elongation appear to be in homologous regions of the face. In the figure green fluorescence highlights the calcein signal administered 30 days prior to sacrifice. The red fluorescent label highlights the alizarin red complexone signal administered 24 hours prior to sacrifice.

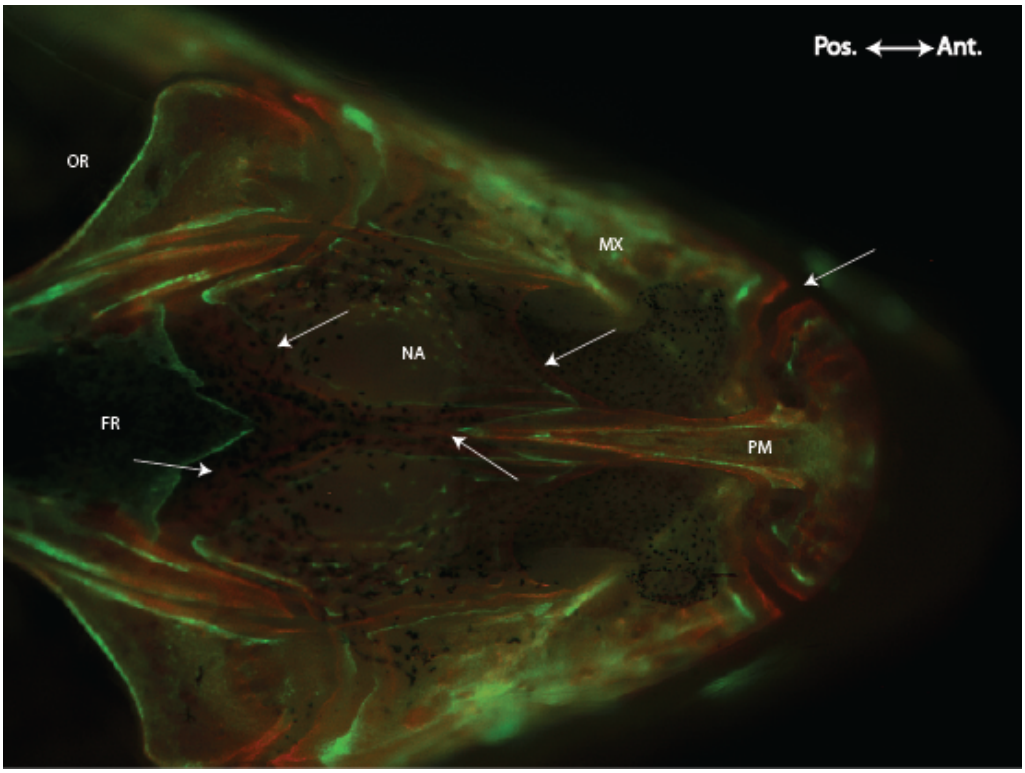

Figure S4: In situ hybridization for the hypertrophic chondrocyte marker *col X*. In contrast to the murine nasal septum there is no evidence of chondrocyte hypertrophy in the anole nasal septum (A, arrows). Note strong expression of *col X* in the hypertrophic chondrocytes of tibial chondroepiphysis (B). The nasal septum is comprised of evenly sized chondrocytes from the anterior-most tip through the length of the face and orbits.

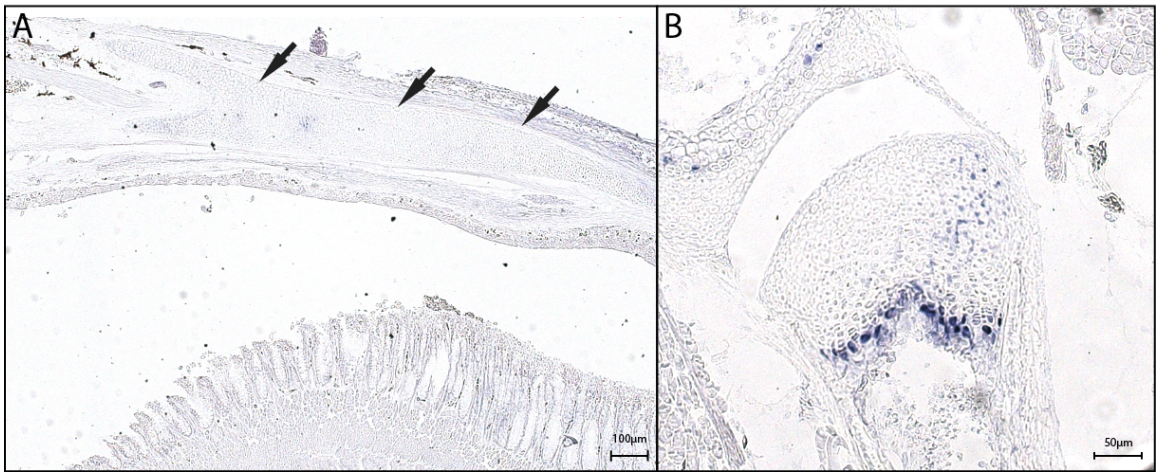

Supplementary Tables

Table S1: Results of PCA on post-cranial morphometric data.
Three significant principal components (PCs, eigen values greater than one) were recovered from analysis of post-cranial variation of 30 anole species. The first PC summarizes variation in lamellae counts on the hands and feet (42%). PC2 summarizes variation in limb length (24%). PC3 summarizes variation in pectoral width (18%). Data were size-corrected prior to analysis.

PC	Eigen Value	Percent Variance	Cumulative variance
1	2.5317	42.194	42.194
2	1.4558	24.263	66.457
3	1.0964	18.273	84.73

Loadings	**PC**		
	1	**2**	**3**
Foot lamellae	**0.86888**	-0.1722	0.36162
Hand lamellae	**0.69656**	-0.42642	0.52921
Forelimb length	0.57309	**0.73638**	0.11133
Hindlimb length	0.58784	**0.67188**	-0.221
Pectoral width	-0.55032	0.20944	**0.61475**
Pelvic width	-0.56094	0.4547	0.49634

Table S2: Results of PCA on cranial geometric morphometric data. Three significant principal components (explaining greater than 5% of the variation) were recovered from geometric morphometric analysis of cranial variation of 30 anole species. Shape changes are consistent with Sanger et al. [2]. PC1 summarizes variation in facial length and width. PCs 2 and 3 explain variation in the size and shape the adductor chambers and braincase. See Sanger et al. [2] for more details.

PC	**Eigen Value**	**Percent Variance**	**Cumulative variance**
1	0.00188585	47.726	47.726
2	0.00072058	18.236	65.962
3	0.00049492	12.525	78.487

Table S3: Summary of cranial and post-cranial dimorphism. Morphometric analyses of cranial dimorphism are consistent with previous analyses presented in Sanger et al [2]. Sample size for post-cranial (PC) and cranial analyses are also presented (female.male).

Species	Sample Size (PC/C)	Post-cranial dimorphism	Cranial dimorphism	Species	Sample Size (PC/C)	Post-cranial dimorphism	Cranial dimorphism
A. aeneus	*5.5/4.3*	0.7343	0.0400	*A. longiceps**	*5.5/2.2*	0.6740	0.0597
*A. allisoni**	*5.5/2.3*	1.0558	0.0721	*A. luciae*	*5.5/1.5*	0.9524	0.0293
A. angusticeps	*5.5/3.4*	0.2337	0.0234	*A. lucius*	*5.5/3.3*	1.1579	0.0153
A. bahorucoensis	*5.5/5.4*	1.4872	0.0645	*A. monticola*	*5.5/5.5*	0.6480	0.0334
A. brevirostris	*5.5/3.6*	0.6450	0.0292	*A. occultus*	*5.5/4.1*	0.3762	0.0129
A. cristatellus	*5.5/7.7*	0.2199	0.0287	*A. oculatus*	*5.5/5.5*	0.4454	0.0460
A. cybotes	*5.5/18.10*	0.7541	0.0417	*A. olssoni*	*5.5/5.6*	0.7796	0.0229
A. distichus	*5.5/16.6*	0.6206	0.0164	*A. opalinus*	*5.5/4.3*	0.4180	0.0126
A. evermanni	*5.5/17.9*	0.2284	0.0252	*A. porcatus**	*5.5/4.8*	1.5736	0.0509
A. garmani	*5.5/3.4*	0.6567	0.0260	*A. richardi*	*5.5/1.3*	0.9066	0.0546
A. grahami	*5.5/12.6*	1.0393	0.0529	*A. roquet*	*6.4/4.5*	0.6871	0.0134
A. griseus	*5.5/3.3*	1.4520	0.0533	*A. sagrei*	*5.5/9.8*	1.1894	0.0312
A. gundlachi	*5.5/1.6*	0.5800	0.0474	*A. sheplani*	*3.3/1.1*	0.9078	0.0398
A. insolitus	*5.5/4.1*	0.8554	0.0508	*A. stratulus*	*5.5/3.4*	1.1064	0.0401
A. krugi	*5.5/3.6*	0.6377	0.0073	*A. valencienni*	*5.5/2.10*	0.5673	0.0507
A. lineatopus	*5.6/4.6*	0.6186	0.0452	*A. wattsi*	*5.5/1.4*	0.5881	0.0371

Next page:

Table S4: Summary of differential expression levels of hormone receptors between males and females of three *Anolis* species with varying levels of facial length dimorphism, between juveniles (juv.), sub-adults (sa.), and adults (ad.). The fold change for the sex with greater relative expression is reported ("M" for male, "F" for female). The most conspicuous difference between male and female *A. carolinensis* at the stage where the sexes are diverging in facial morphology is in the relative expression of estrogen receptor beta. This difference is not present at juvenile stages and is not found in the other anole species examined. The number of males and females is also noted for each comparison.

***A. carolinensis* juvenile (6M/6F)**		
	Fold Change	**p-value**
AR	1.59M	0.320
IGFr1	1.10F	0.644
Erβ	1.29F	0.438
Erα	1.27F	0.200
PTH1r	1.09F	0.643
GHr	2.09M	0.075

***A. sagrei* juvenile (5M/5F)**		
	Fold Change	**p-value**
AR	1.23F	0.407
IGFr1	1.48F	0.333
Erβ	1.30F	0.462
Erα	1.17M	0.194
PTH1r	1.01M	0.938
GHr	1.42F	0.418

***A. cristatellus* juvenile (4M/4F)**		
	Fold Change	**p-value**
AR	1.77M	0.396
IGFr1	1.04M	0.881
Erβ	1.10F	0.778
Erα	1.06M	0.835
PTH1r	1.57M	0.338
GHr	1.28M	0.366

***A. carolinensis* subadult (6M/5F)**		
	Fold Change	**p-value**
AR	1.03M	0.847
IGFr1	1.49F	0.081
Erβ	**4.44F**	**p<0.001**
Erα	1.12F	0.357
PTH1r	1.09M	0.689
GHr	1.45F	**0.015**

***A. sagrei* subadult (5M/5F)**		
	Fold Change	**p-value**
AR	1.24M	0.201
IGFr1	1.17F	0.428
Erβ	1.27M	0.558
Erα	1.01M	0.954
PTH1r	1.43M	0.104
GHr	3.50M	0.102

***A. cristatellus* subadult (6M/5F)**		
	Fold Change	**p-value**
AR	1.50M	0.181
IGFr1	1.63F	0.221
Erβ	1.65F	0.200
Erα	1.50F	0.388
PTH1r	1.63F	0.201
GHr	1.61F	0.121

***A. carolinensis* adult (6M/6F)**		
	Fold Change	**p-value**
AR	1.53M	0.067
IGFr1	1.26M	0.127
Erβ	**11.2F**	**p<0.001**
Erα	1.20M	0.143
PTH1r	1.28M	0.184
GHr	1.27M	0.187

***A. sagrei* adult (6M/5F)**		
	Fold Change	**p-value**
AR	1.15F	0.381
IGFr1	1.17F	0.311
Erβ	1.06F	0.811
Erα	1.19M	0.052
PTH1r	1.11F	0.543
GHr	1.59M	0.061

***A. cristatellus* adult (6M/6F)**		
	Fold Change	**p-value**
AR	1.17M	0.111
IGFr1	1.05F	0.909
Erβ	2.43M	0.066
Erα	1.16M	0.556
PTH1r	2.66M	0.060
GHr	1.10M	0.657

Table S5: Differential expression levels for hormone receptors and accessory molecules in the chondroepiphyses of adult male and female *A. carolinensis*. Note that there are no significant differences in expression indicating that the differential expression of estrogen receptor beta is face specific. The fold change for the sex with greater relative expression is reported ("M" for male, "F" for female).

***A. carolinensis* chondroepiphyses**		
Gene	**Fold Change**	**p-value**
ar	1.58F	0.528
Igfr1	1.07M	0.714
erβ	2.49F	0.318
erα	1.04M	0.943
pth1r	1.02M	0.957
ghr	1.29F	0.579
5α-reductase	1.13F	0.851
Aromatase	1.54F	0.789
src1	1.33F	0.561
cbp	1.47M	0.178
foxo1	1.14F	0.478
igfbp5	1.79M	0.436

Table S6: Summary of differential expression levels between males and females of *A. carolinensis* for molecules involved with metabolizing or activating the steroid and IGF pathways in juveniles (juv.), sub-adults (sa.), and adults (ad.). The fold change for the sex with greater relative expression is reported ("M" for male, "F" for female). The subtle differences in expression during the subadult stage are likely due to differences in the precise timing of sexual maturation between males and females. It remains unclear whether the expression differences observed at the subadult stage represent differences in the timing of sexual maturation between males and females or organizational effects [10], establishing the cellular parameters that effect later growth.

***A. carolinensis* juvenile**				
	Function	**Pathway**	**Fold**	**p-value**
5α-reductase	Metabolic enzyme	Steroid	1.098F	0.806
Aromatase	Metabolic enzyme	Steroid	1.06F	0.726
src1	Nuclear coactivator	Steroid	1.03F	0.868
cbp	Nuclear coactivator	Steroid	1.47M	0.220
foxo1	Transcription factor	IGF	1.20F	0.505
igfbp5	Carrier Protein	IGF	1.12M	0.770
***A. carolinensis* subadult**				
	Function	**Pathway**	**Fold**	**p-value**
5α-reductase	Metabolic enzyme	Steroid	1.73M	0.071
Aromatase	Metabolic enzyme	Steroid	**2.21F**	**0.022**
src1	Nuclear coactivator	Steroid	**1.57F**	**0.048**
cbp	Nuclear coactivator	Steroid	**3.35F**	**p<0.001**
foxo1	Transcription factor	IGF	1.14F	0.478
igfbp5	Carrier Protein	IGF	**1.34M**	**0.030**
***A. carolinensis* adult**				
	Function	**Pathway**	**Fold**	**p-value**
5α-reductase	Metabolic enzyme	Steroid	1.53F	0.051
Aromatase	Metabolic enzyme	Steroid	1.24F	0.418
src1	Nuclear coactivator	Steroid	**1.74F**	**0.010**
cbp	Nuclear coactivator	Steroid	1.62F	0.090
foxo1	Transcription factor	IGF	1.21M	0.405
igfbp5	Carrier Protein	IGF	1.33M	0.219

Table S7: Comparison of juvenile and adult expression levels for hormonal receptors for three *Anolis* species. Note that the relative levels of most hormone receptors decreases with age in each species. ERβ exhibits a distinct pattern in each species, but only in *A. carolinensis* is this receptor differentially regulated in males and females, being significantly upregulated in females and significantly downregulated in males. The fold change for the stage with greater relative expression is reported ("J" for juvenile, "A" for adult).

***A. carolinensis* temporal analysis**					
Male			**Female**		
Gene	**Fold Change**	**p-value**	**Gene**	**Fold Change**	**p-value**
ar	1.60A	0.136	*ar*	1.67A	0.121
Igfr1	1.71J	0.152	*Igfr1*	1.87J	**0.007**
*er*β	**2.19J**	**0.019**	*er*β	**3.97A**	**p<0.001**
*er*α	**1.63J**	**0.029**	*er*α	**2.31J**	**p<0.001**
pth1r	**1.72J**	**0.044**	*pth1r*	**2.02J**	**p<0.001**
ghr	**5.27J**	**0.011**	*ghr*	**3.19J**	**p<0.001**
***A. cristatellus* temporal analysis**					
Male			**Female**		
Gene	**Fold Change**	**p-value**	**Gene**	**Fold Change**	**p-value**
ar	**7.80J**	**0.02**	*ar*	5.19J	0.051
Igfr1	1.49J	0.167	*Igfr1*	1.36J	0.471
*er*β	**9.74A**	**0.026**	*er*β	**3.67A**	**p<0.001**
*er*α	1.31A	0.321	*er*α	1.20A	0.518
pth1r	**11.80J**	**0.014**	*pth1r*	**19.90J**	**p<0.001**
ghr	**3.25J**	**0.001**	*ghr*	**7.81J**	**0.006**
***A. sagrei* temporal analysis**					
Male			**Female**		
Gene	**Fold Change**	**p-value**	**Gene**	**Fold Change**	**p-value**
ar	**2.28J**	**p<0.001**	*ar*	**2.44J**	**0.025**
Igfr1	**2.89J**	**0.002**	*Igfr1*	3.63J	0.069
*er*β	**2.06J**	**0.046**	*er*β	**2.53J**	**0.005**
*er*α	**1.99J**	**p<0.001**	*er*α	**2.03J**	**0.002**
pth1r	**1.84J**	**0.008**	*pth1r*	**1.64J**	**p<0.001**
ghr	2.71J	0.062	*ghr*	**6.12J**	**0.044**

Table S8: List of qPCR primer sequences

Control Genes	Symbol	Forward primer	Reverse primer
Beta-actin	ACTB	CATTCAACACTCCAGCCA	CACCATCTCCAGAGTCCA
Glyceraldehyde-3-phosphate dehydrogenase	GAPDH	CAGAACATCATCCCAGCA	AGGTCCACAACGGAAACA
Receptors	**Symbol**	**Forward primer**	**Reverse primer**
Androgen receptor	AR	ATGTGGTGAAATGGGCAA	AAGTAGAGCATCCGAGAG
Estrogen receptor alpha	Erα	AATGACACTGCTAACCAACC	CACACCAAGCCAACCATC
Estrogen receptor beta	Erβ	TTGCACCAGACCTAGTCCTAGACA	CTCGCAGTCTTGAAGTTGTTGCCA
Insulin-like growth factor receptor 1	IGFr1	GGCGAAAGAGTGTGGAGA	TCGGTGCAAGCGTATTTG
Growth hormone receptor	GHr	CACTCAACTACCACCTCC	AACTCCCCATAAACTCCC
Parathyroid hormone-related protein 1 receptor	PTH1r	CTTTCCAGGGATTTTTCGT	TCCGTAGCTGTAGGTGGT
Accessory Molecules	**Symbol**	**Forward primer**	**Reverse primer**
5α-reductase	SRD5A1	CAGAAAACCAGGAGAGACA	CAAGAGCAAATCCAAACCA
Aromoatase	ARO	TTATGAGGCGGGTTATGCTGGACA	CTTAAAGAAGATATCGGGTTTCAGCAG
Nuclear receptor co-activator 1	SRC1	GCTCCTCCGCTACCTTCTTGA	GGGTTAGACGCCAGCTCCTT
CREB-binding protein	CBP	GCACCGTCTGCGAGGATT	TCTTAGCGTTGTAGCAGTTGATGC
Insulin-like growth factor-binding protein 5	IGFbp5	AAAAAGGATCGCAGGAAGAA	CGCTGGCTTGATTTTAGT
Forkhead box protein O1	FOXO1	CAAGAACGTGCCCTACTTCAA	TGCTGTGTAATGAGAGGTTGTG

Alternative primers used in comparatative analyses

Receptors	Symbol	Forward primer	Reverse primer
Parathyroid hormone-related protein 1 receptor (A. cristatellus)	PTH1r	CTTTCCAGGGTTTTTTTGT	As above
Insulin-like growth factor receptor 1 (A. cristatellus, A. sagrei)	IGFr1	ACATGGTGGACGTGGACCTGCC	GTG ACG GCT TTG ACA TAA ATG GCG
Androgen receptor (A. cristatellus, A. sagrei)	AR	ACC ATC GAC AAG TTC CGG CGG	GCATCTTCAGGTTGCCCAG

Author contributions:

TJS, JBL, and AA conceived of and designed the project
AA and JBL supervised and funded the project
TJS and SMS collected skeletal tissues and processed cDNA
TJS and SMS collected wild caught specimens and captively bred juvenile lizards
TJS and SMS optimized qPCR primers and performed gene expression analyses
TJS cloned hormonal receptor in situ probes
TJS performed the facial growth pulse labeling study
MT performed proliferation analysis
RBL and LMS collected and analyzed postcranial morphometric data

All authors contributed to the preparation of the manuscript. TJS produced all figures and tables.

Supplementary References

1 Klingenberg, C. P. 2010 Evolution and development of shape: integrating quantitative approaches. *Nat. Rev. Genet.* **11**, 623–35.

2 Sanger, T. J., Sherratt, E., McGlothlin, J. W., Brodie, E. D., Losos, J. B. & Abzhanov, A. 2013 Convergent evolution of sexual dimorphism in skull shape using distinct developmental strategies. *Evolution* **67**, 2180–93.

3 Rohlf, F. 2006. tpsDig, version 2.10. Department of Ecology and Evolution, State University of New York, Stony Brook, NY.

4 Klingenberg, C. P. 2011 MorphoJ: an integrated software package for geometric morphometrics. *Mol. Ecol. Resour.* **11**, 353–7.

5 Klingenberg, C. P., Barluenga, M. & Meyer, A. 2002 Shape analysis of symmetric structures: quantifying variation among individuals and asymmetry. *Evolution* **56**, 1909–20.

6 Alföldi, J. et al. 2011 The genome of the green anole lizard and a comparative analysis with birds and mammals. *Nature* **477**, 587–91.

7 Sanger, T. T. J., Mahler, D. L., Abzhanov, A. & Losos, J. J. B. 2012 Roles for modularity and constraint in the evolution of cranial diversity among *Anolis* lizards. *Evolution* **66**, 1525–1542.

8 Sanger, T., Hime, P., Johnson, M., Diani, J. & Losos, J. B. 2008 Laboratory protocols for husbandry and embryo collection of Anolis lizards. *Herpetol. Rev.* **39**, 58–63.

9 Livak, K. J. & Schmittgen, T. D. 2001 Analysis of relative gene expression data using real-time quantitative PCR and the 2(-Delta Delta C(T)) Method. *Methods* **25**, 402–8.

10 Adkins-Regan, E. 2012 Hormonal organization and activation : Evolutionary implications and questions. *Gen. Comp. Endocrinol.* **176**, 279–285.